

State Space Assessment on the Impact of Sea Surface Temperature on Fishing Effort in Continental US Exclusive Economic Zones

Mingzhao Hu^{1,*} and Qutu Jiang²

¹*Department of Statistics and Applied Probability,
University of California, Santa Barbara, California, USA*

²*Department of Geography, The University of Hong Kong, Hong Kong, China*

Correspondence*:

Mingzhao Hu
mingzhaohu@ucsb.edu

2 ABSTRACT

3 Fishing effort reflects the investment strategies and costs of the industry participants, which is
4 essential to coastal livelihoods and seafood security. Recent changes in marine environments
5 are expected to influence human fishing activities. Yet, how sea surface temperature (SST) alter
6 fishing effort has been rarely studied. In this study, we applied a dynamic spatiotemporal model
7 in the state space framework to explore the relationship between SST and fishing effort with
8 advanced satellite-derived high resolution data in the exclusive economic zone of continental
9 United States. Results show a positive relationship between SST and fishing effort in both east
10 and west coast of United States, that is, more fishing activities in warmer waters. Furthermore, a
11 forecast of fishing effort for one year is implemented using the proposed dynamic model, which
12 would guide climate policy-making and fishing strategies.

13 **Keywords:** dynamic spatiotemporal model, stochastic partial differential equation, integrated nested Laplace approximation, fishing
14 effort, sea surface temperature, exclusive economic zone

1 INTRODUCTION

15 In today's world, fishery is of increasing concern as it is an industry at the intersection of environmental
16 protection, national economy and global food security. With recent advances in satellite imaging and
17 tracking technology, a consistent global monitor of fishing vessels on a daily level became available
18 for the first time. We propose to consider the dynamic evolution in time of global fishing activities in
19 response to environmental factors across different locations via a state space approach that handles large
20 datasets in a computationally feasible manner. To this end, we model the spatiotemporal covariance with a
21 Gaussian Markov Random Field (GMRF), which is constructed by stochastic partial differential equations
22 (SPDE), and adopt integrated nested Laplace approximation (INLA) for parameter estimation. We apply
23 this approach to an extensive novel dataset and investigate how fishing effort in the exclusive economic zone
24 (EEZ) of continental United States are affected by the sea surface temperature. This not only demonstrates
25 the flexibility of these spatiotemporal dynamic models on a larger and more detailed geographical scale,
26 but more importantly, provides quantitative conclusions that assist in making future commercial fishing
27 plans and environmental regulations.

The following sections are organized as follows. Section 1.1 introduces the datasets recording the fishing effort and the sea surface temperature. Section 1.2 outlines the main statistical challenges and the contributions of this project. Section 1.3 presents the research questions and objectives. Section 2 constructs the dynamic spatiotemporal model based on the general situation. Section 2.1 discusses the SPDE representation of the GMRF in modeling the spatial dependence of data and introduces the INLA approach for inference. Section 3 presents exploratory data analysis, including discussions on the projection of global data in coordinates, the spherical distance and covariance, and the global fishing effort based on EEZ. Section 4 presents applications of the proposed methodology to the real-life fishing effort data. Section 5 discusses our findings as well as future research.

1.1 Introduction to Data

The main focus is on fishing activities in the exclusive economic zone (EEZ) of each country, since this is one of the two main disciplines of fishing, the other being high seas fishery. The focus is on the fishing effort by each country in its own EEZ. Most commercial fishery data sources are hindered by concerns for private corporate information, and public data is mostly on species at annual and country level, such as the fisheries and aquaculture data published by the United Nations Food and Agriculture Organization (FAO, 1967). The few public sources that can link fisheries data to specific geographical locations are limited to specific regions. Moreover, the individual vessel information recorded in the GFW (GFW, 2018) data holds the potential for research into movement of fishing vessels, tracking, etc.

Global sea surface temperature is collected from the Optimum Interpolation Sea Surface Temperature dataset (Banzon et al., 2020) which is publicly available from National Centers for Environmental Information under NOAA. The original data in Optimum Interpolation Sea Surface Temperature (OISST) consists of 0.25 degrees latitude by 0.25 degrees longitude grid cells and is gathered from different platforms, including satellites, ships, buoys, etc., which has provided it with better coverage and cross-referenced accuracy. The missing geographical components are interpolated with considerations for bias adjustments. Using the daily sea surface temperature, we select the Advanced Very High Resolution Radiometer (AVHRR) data generated via infrared instruments for its higher resolution and inclusion of land-adjacent areas. The grid cells and actual geographical regions from the GFW (GFW, 2018) and OISST (Banzon et al., 2020) datasets are carefully cleaned and matched before our explorations in Section 3 and Section 4.

1.2 Challenges and Novelties

First and foremost, the novel data from GFW (GFW, 2018) presents challenges in data manipulations. The fishing hours are aggregated into grids of 0.01 degree of latitude by 0.01 degree of longitude, hence the first challenge in the following analysis is recognizing that these should not be treated as point referenced data. For each entry in *fishing_hours*, it gives the fishing effort measured in hours by all vessels of that country while inside that grid. Furthermore, the grids are irregular since they are measured in degrees of longitude and latitude. Because the Earth is an ellipsoid, the longitudes change from 111 km for 1 degree at the equator to 0 at the poles. The latitudes also vary from 110.567 km at the equator to 111.699 km for one degree at the poles. For simplicity, in the following analysis we will assume the Earth is a perfect sphere.

The second challenge is that all data are recorded in spherical coordinates since this is a global data set. Unlike regional data, for example, one limited to California, in this case one cannot ignore the surface curvature of the Earth. The critical choice of an appropriate projection is discussed in Section ??.

69 Some other challenges for data analysis are due to the size of the data which leads to higher cost in
70 manipulation. Part of the solution is to carefully filter the data in preparation so as to discard unnecessary
71 information such as vessel presence and integrate to suitable spatial and temporal scale. Furthermore, as a
72 relatively recent source, Global Fishing Watch (GFW, 2018) only started in 2012. The lack of historical
73 data will be a concern in research on the spatiotemporal scale.

74 Modeling the dynamic evolutions along time needs to consider the spatial covariance structure, and the
75 computational feasibility is challenged not only by the filtering process in the dynamic models, but also the
76 complexity of the covariance which is considered in general as a Gaussian field. Finding efficient ways for
77 the inference of the parameters in our dynamic models is a vital component in reducing complexity.

78 Despite these obstacles, this is an unparalleled opportunity to consider fishery at specific locations on a
79 global and daily scale. To begin with, the fisheries data is collected at detailed, specific locations across the
80 globe over continuous time for each day in the year. This provides the potential for a dynamic approach
81 on a larger geographical scale and with more details. To the best of our knowledge, there has been no
82 application of dynamic models in fisheries studies on such a comprehensive spatial and temporal level. In
83 addition, each fishing vessel is identified with AIS, allowing for future research into movement, tracking,
84 etc.

85 More importantly, the state space model captures the dynamic evolution, therefore in considering
86 the influence of sea surface temperature on fishing efforts, the year-over-year and month-over-month
87 comparisons are more informative. The proposed modeling framework is available for advising commercial
88 fishing operations on predicting peak fishing period and hotspots to maximize revenue. In addition, it
89 provides assistance in making governmental guidelines on fishing activities to minimize overfishing and
90 other illegal fishing activities to preserve the marine living resources and ecosystem balance.

91 1.3 Research Questions

92 This project aims at addressing the following concerns. First, we propose to model the dynamic influence
93 of sea surface temperature on fishing efforts when both spatial locations and temporal progressions are
94 considered. This is one of our main contributions and provides quantitative support for fishing-related
95 decision-making with new details revealed from the global activities.

96 Second, we aim to develop a computationally feasible model for this purpose given a large dataset. This
97 is the focus of Section 2.

98 Third, we interpret the economic and environmental revelations from studying how fishing efforts in EEZ
99 along the Atlantic coast of US dynamically relates to sea surface temperature, versus that of the Pacific
100 coast. This extra factor of comparison in addition to sea surface temperature is reflected in our design of
101 implementation.

102 Moreover, prediction and interpolation based on geographical location can be found for guiding future
103 fishing activities. While the effort in fishing at different locations is very much due to subjective human
104 decision of the crew, it is still influenced by factors such as cost, revenue, stock assessment and government
105 policy such as subsidy and moratorium. Having a means to estimate future fishing effort at a location serves
106 as another factor in helping participants in the fishing industry make the most beneficial plan to allocate
107 their resources and effort.

2 DYNAMIC SPATIOTEMPORAL MODEL

108 Longitudinal variables are ones that contain repeated measurements of time. To model the dynamic process
 109 of a longitudinal variable changing with respect to another longitudinal variable over a region, state
 110 space models, also known as dynamic linear models, are especially advantageous and offer a unified
 111 methodology on a system assumed to be determined by unobserved state vectors. More specifically, the
 112 dynamic evolution of fishing effort in response to sea surface temperature is a special application. The
 113 proposed modeling framework in Section 2 accommodates all spatiotemporal data analysis and is not
 114 limited to research topics in fisheries. There have been discussions on implementing dynamic linear models
 115 for spatiotemporal data 2001 (Stroud et al., 2001; Lindström et al., 2014; Hefley et al., 2017), but to
 116 accommodate the scale of global and daily data in a computationally feasible manner, in Section 2 we
 117 adopt the framework of Godana et al (Godana et al., 2019). We will now introduce the state space model
 118 setup.

119 Let $Y(s, t)$ be the spatiotemporal process of the longitudinal variable of interest at time point t and
 120 location s , and assume the model

$$Y(s, t) = \beta Z(s, t) + \Phi(s, t) + \epsilon(s, t), \quad (1)$$

121 which is spatially and temporally independent, $Z(s, t)$ is the covariates, $\Phi(s, t)$ is the latent states, and
 122 the white noise $\epsilon(s, t)$ is serially and spatially independent, following $N(0, \sigma_\epsilon^2)$. The latent states evolves
 123 dynamically via

$$\Phi(s, t) = \lambda \Phi(s, t - 1) + \gamma(s, t), \quad (2)$$

124 which is spatially and temporally independent. $\Phi(s, 1)$ follows $N(0, \frac{\sigma_\gamma^2}{1-\lambda^2})$ and $\gamma(s, t)$ independently
 125 follows $N(0, \sigma^{2*})$.

126 The parameters are given by $\Theta = (\beta, \lambda, \sigma_\epsilon^2, \sigma_\gamma^2, \kappa)$. Furthermore, the joint posterior of the
 127 parameters, $P(\Theta, \Phi|Y)$, is the product of the data model, process model, and parameter model,
 128 $P(Y|\Theta, \Phi)P(\Phi|\Theta)P(\Theta)$. This can be determined under a Markovian process assumption and independent
 129 hyperparameters assumption.

130 Note that for equation (2), σ^{2*} is a spatiotemporal covariance that is sensitive to the number of
 131 geographical locations and time points. When the data is comprehensive, to avoid issues with computational
 132 feasibility, we introduce the following stochastic partial differential equation approach.

133 2.1 Stochastic Partial Differential Equation (SPDE) Approach

134 We shall first define the spatiotemporal covariance σ^{2*} explicitly

$$\begin{aligned} \sigma^{2*} &= Cov(\gamma(s, t), \gamma(s', t')) \\ &= \sigma_\gamma^2 1_{(t=t', s=s')} + \sigma_\gamma^2(r) 1_{(t=t', s \neq s')}, \end{aligned} \quad (3)$$

135 where $1_{(.)}$ is the indicator function, and σ_γ^2 is defined by Matern on the spatial distance r

$$C(r) = \frac{1}{\Gamma(\nu)2^{\nu-1}} (kr)^\nu \kappa_\nu(kr), \quad (4)$$

136 and κ_ν is the modified Bessel function of the second kind, ν is the smoothness parameter, k is the scaling
 137 parameter and range $\rho = \frac{\sqrt{8\nu}}{k}$. In the following, ν is specified to 1.

138 Spatial dependence of areal units may be modeled by a Gaussian Markov random field (GMRF), which
 139 is a multivariate $N(0, Q)$ distribution, with sparse precision matrix Q . This sparsity gives a significant
 140 computational advantage. For a Matern field $X(s)$ with domain D_s , i.e. a second order stationary and
 141 isotropic Gaussian field with Matern covariance, we adopt the SPDE approach to define the Matern field
 142 as a linear combination of the basis based on a triangulation of the domain. If given a pseudodifferential
 143 operator $(\kappa^2 - \Delta)^{\frac{\alpha}{2}}$ with $\alpha = \nu + \frac{m}{2}$, $\kappa > 0$, $\nu > 0$, $\Delta = \sum_{i=1}^m \frac{d^2}{dx^2}$, then the Matern Field $X(s)$ is a
 144 solution to the stochastic partial differential equation (SPDE)

$$(\kappa^2 - \Delta)^{\frac{\alpha}{2}} X(s) = \omega(s), \quad (5)$$

145 where $\omega(s)$ is white noise following spatial $N(0, 1)$. Furthermore, given a triangulation, basis functions
 146 defined on the triangulation ψ_j , and the Matern field as the solution to the SPDE $X(s)$, we have

$$X(s) = \sum_{j=1}^k w_j \psi_j(s), \quad (6)$$

147 where the weights (w_1, \dots, w_k) are a GMRF. γ_t in the dynamic spatiotemporal models is a Matern Field
 148 that can now be specified with a GMRF with precision matrix Q_s via the SPDE approach. The dynamic
 149 spatiotemporal model (2) becomes

$$\begin{aligned} Y(s, t) &= \beta Z(s, t) + \sum_{i=1}^n H_{ij} \Phi(s, t) + \epsilon(s, t), \\ \Phi(s, t) &= \lambda \Phi(s, t-1) + \gamma^*(s, t), \end{aligned} \quad (7)$$

150 where $H_{ij} = 1_{(\text{Triangulation vector } j \text{ is placed at location } i)}$, and $\gamma^*(s, t)$ now follows $N(0, Q_s^{-1})$, $\Phi(s, 1)$ follows
 151 $N(0, \frac{Q_s^{-1}}{1-\lambda^2})$.

152 We implement the integrated nested Laplace approximation (INLA) to compute the dynamic model.
 153 INLA (Rue et al., 2009) is a computational Bayesian procedure to approximate the posterior marginals
 154 of the latent states and the hyperparameters. In implementing INLA, we write the observation equation in
 155 matrix form, then stack the simple model building blocks into large complicated models. The details of the
 156 procedure may be found in Rue et al (Rue et al., 2009). In Section 4, we adopt R-INLA 5 (Blangiardo and
 157 M., 2015) in model computations.

158 The framework is specifically designed to be computationally efficient and flexible for accommodating
 159 different spatiotemporal datasets. In the following sections, we consider the novel GFW (GFW, 2018)
 160 dataset as a special case for implementing the proposed dynamic model and investigate the influence of the
 161 covariate, sea surface temperature.

3 EXPLORATORY DATA ANALYSIS

162 We begin with some necessary assumptions for the GFW (GFW, 2018) dataset. Gaussianity and isotropy are
 163 assumed along with the previous assumption that the Earth is a sphere. These are not perfect representations

165 of the real-life situation, but simplify the discussion and reduce the number of obstacles in the following
166 analysis.

167 The original gridded fishing effort and oceans were initially recorded in degrees of longitude and latitude
168 under GPS coordinates projection. Hence, the grids are irregular and this increases difficulty in spatial
169 analysis. For completeness and to ensure the appropriate projection of spherical data onto 2D plots, they
170 are reprojected using a Gall-Peters Equal Area Projection. Gall-Peters Equal Area Projection is a map
171 projection that was first introduced by Gall (Gall, 1885). As a rectangular map projection, it sacrifices
172 surface features of the Earth in the tropics and poles but preserves the relative sizes. Given the Earth radius
173 R , longitude (from central meridian) λ , and latitude θ , the projection is

$$\begin{aligned} x &= \frac{R\pi\lambda}{180^\circ\sqrt{2}}, \\ y &= \sqrt{2}R\sin(\theta). \end{aligned} \quad (8)$$

174 The construction of plots in the following sections are all in Gall–Peters Equal Area Projection, but for
175 ease of understanding, the resulting transformed coordinates are still referred to as longitude and latitude.
176 In analysis, it remains an issue to correctly calculate the spherical distances and covariances. We look for
177 the great-circle distance, which is the shortest length between two points along the surface of the sphere, in
178 kilometers for each pair of locations of nonzero fishing effort in corresponding EEZ by country. When
179 given radius R , longitude λ_1, λ_2 , latitude θ_1, θ_2 , the great-circle distance is

$$d = R\arccos(\sin\theta_1\sin\theta_2 + \cos\theta_1\cos\theta_2\cos(|\lambda_1 - \lambda_2|)), \quad (9)$$

180 where using *Rdist.earth* function from R package “fields” (Douglas Nychka et al., 2021), we found that
181 in the GFW (GFW, 2018) dataset the minimum spherical distance of each location to other locations
182 with nonzero fishing effort is from 1.1 km to 410.4 km. This discovery suggests that these locations with
183 observed fishing activity are relatively close, partly due to the constraint of exclusive economic zones. Also
184 there is considerable variations between these spherical distances, with some nearest-location pairs next to
185 each other, others hundreds of kilometers away. Therefore, a quantitative tool for predicting the fishing
186 effort at any given location and time would help ship crew determine the allocation of fishing resources.

187 Several spherical covariance functions have been recently proposed, such as by Gribov and Esri (Gribov
188 and Krivoruchko, 2018), and by Porcu et al (Porcu et al., 2017). One way is to compute the isotropic
189 spherical covariance on a compact support. Given the spherical distance d and the range of support ϕ , the
190 covariance is

$$C(d) = (1 - \frac{3d}{2\phi} + \frac{1}{2}(\frac{d}{\phi})^3)1_{\{0 \leq d \leq \phi\}}, \quad (10)$$

191 where ϕ is the range. This isotropic spherical covariance is defined on a compact support, which is similar
192 to the covariance proposed by Porcu et al (Porcu et al., 2017). Constraining to an appropriately small area
193 within the range ϕ suggests that the surface curvature can be ignored for simplicity.

194 For our project, the interest is on the fishing effort within the exclusive economic zone, which is the
195 area within 200 nautical miles from the territorial coastline. The EEZ boundaries are obtained from
196 Marineregions.org (Mar, 2019). Figure 1 suggests that the fishing activities in the United States EEZ seem
197 to concentrate in the Pacific Northwest, the Mexican Gulf, and New England. Also, the color of grid cells
198 are predominantly light green, with occasional instances of warmer colors indicating higher fishing effort
199 per square km. The concentration of fishing effort values in a relatively short interval resulted in most

grid cells sharing similar color, which indicates that the grid-wise variation is insignificant relative to the maximum fishing effort. On the other hand, popular fishing grounds, such as Newfoundland, North Sea and the Japanese Sea are more distinguishable. For a comparison between countries, we report that China has significantly higher total fishing hours than any other country by a large margin, and France also stands out from the rest. The fishing effort in EEZ by country is very different from that of total fishing effort. Even within the top seven countries, the per square km fishing hours is hugely different, ranging from over 1200 to below 100. Similarly, the annual changes are vastly different for different countries. By adding a temporal dimension to the spatial analysis of fishing effort, we can now consider a dynamic point of view. This calls for establishing a dynamic model that is more appropriate for the purpose of guiding ongoing and future commercial fishery activities and related economic policies.

4 IMPLEMENTATION RESULTS

In this section, we apply the models from Section 2 to the GFW (GFW, 2018) dataset. We begin with more data wrangling for continental US EEZ. We first select fishing hours from 2012 to 2018 in 0.01 by 0.01 degree grids, then import EEZ boundaries for east coast and west coast of continental US separately as polygons. After importing sea surface temperature data from NOAA, it is matched with fishing hours by location into grids of 1 degree latitude by 1 degree longitude, for each week from 2012 to 2018. This reduces computational complexity yet retains sufficient information to reflect geographical and seasonal variations. Furthermore, to address the third research question and compare between the EEZ on the Atlantic coast and the Pacific coast, we divide the data into two subsets.

Mesh constructs the triangulation of the domain for the basis functions and the figures below shows the results. There is a tradeoff between computation cost and estimation accuracy. Having more triangles achieves higher accuracy, but would take longer to compute. The desired mesh would have smaller triangles where the original data is dense and larger triangles where the original is more sparse.

In Figure 2 and Figure 2, the blue lines show the boundaries of the EEZ and the red dots indicate the grid cells. The mesh is desirable and achieves a good balance between computation cost and estimation accuracy. INLA produced the following estimated observation equations,

$$Y(s, t) = 59.93 + 4.32Z(s, t) + \Phi(s, t) + \epsilon(s, t), \text{ for east coast}, \quad (11)$$

for the east coast, and

$$Y(s, t) = 27.57 + 3.59Z(s, t) + \Phi(s, t) + \epsilon(s, t). \quad (12)$$

for the west coast. Overall both observation equations show a positive relationship between the sea surface temperature and fishing effort, which echoes previous research in literature that in general warmer waters and seasons correspond to more fishing activities along both the east and west coast of United States. At the same time, given the same conditions, the east coast would have higher fishing hours. The rest of the posterior estimates of parameters are given in Table 2. The most significant difference between posterior estimates for the two coasts is the variation for the white noise in the observation equation for east coast is considerably higher than for west cost. These posterior estimates and densities for the parameters can be visualized in Figure and Figure below, where the red line indicates the expected value of the parameter. The variance, β , κ and the range ρ are represented here and the posterior densities are reasonable. Based on these, we continue to carry out the predictions for fishing effort separately for the east coast and the west coast EEZ. To save space and for better presentation, only the first week of each month is selected in Figure 6 and 7

238 In Figure 6 featuring the one-year-ahead prediction for east coast fishing effort based on location, time
239 and sea surface temperature, there is relatively more lighter colored grid cells in the summer months.
240 Activities concentrate in the Northeast and Southwest, corresponding to New England and the Mexican
241 Gulf. For the west coast, fishing activities are also more common in the summer, while concentration
242 is in the Pacific Northwest. These results echo previous research in the literature and demonstrate the
243 effectiveness of the dynamic spatiotemporal model in providing useful predictions based on the novel GFW
244 (GFW, 2018) dataset.

5 DISCUSSION

245 We have incorporated covariate effects in a dynamic spatiotemporal model and studied how fishing effort
246 is related to sea surface temperature. The dynamic perspective is more suitable for capturing the nature
247 of shifting temperature in different time and place, therefore it is a more accurate representation of this
248 relationship. The dynamic models are implemented via a computationally efficient approach which consists
249 of solving SPDE and implementing INLA in R. We introduced GMRF to model the spatiotemporal
250 covariance and the resulting sparsity improved the computations. INLA further simplifies the inference
251 process.

252 Using novel global fishing dataset at a more detailed geographical and temporal level than previous
253 fishery studies, this project reveals that fishing effort is positively related to sea surface temperature, with
254 the east coast EEZ having more fishing hours if under the same conditions. The model provides reasonable
255 predictions for fishing effort and highlights the environmental influence for commercial fishing. Given the
256 variations in fishing hours reflected by the model and illustrations, future conservation efforts regarding
257 fishing regulations may take into account not only the specific location and time, but also the sea surface
258 temperature when analyzing expected fishing activities. A realistic prognosis is vital in determining the
259 balance between economic profit and sustainable development.

260 For future research, computational efficiency is key in dealing with large spatial datasets. We hope to
261 explore alternative strategies to outperform the current SPDE approach, and compare the performances. As
262 another possible improvement, some assumptions do not adequately reflect reality, and further attempts
263 should be made to relax them. For example, we would like to consider extending the dynamic model to
264 the nonGaussian case. This requires numerical approximations of the nonGaussian case as a Gaussian,
265 therefore adding to the computational burden. Furthermore, the model has the potential to incorporate
266 more covariates such as vessel types, fish species, etc. The GFW (GFW, 2018) dataset also includes further
267 fishery variables for consideration. Actual policy making calls for a more extensive consideration based on
268 the current dynamic model. We may expand to more longitudinal variables in addition to fishing effort.

269 Cutting-edge remote sensing technology has greatly improved big data for earth observation. Records
270 of fishing activities in near real-time are essential for preserving our oceans and promoting sustainability.
271 In this project, we have introduced and implemented rigorous spatiotemporal methodologies that offers a
272 dynamic perspective on human fishing effort, providing a data-based platform for the prediction of fishing
273 hours and a comparison between patterns in continental United States EEZ. In the process, we also provide a
274 quantitative understanding of the marine environment attributes which reports the spatiotemporal variations.
275 These measures contribute to environmental protection management that not only enable sustainability, but
276 also promote the public good.

CONFLICT OF INTEREST STATEMENT

277 The authors declare that the research was conducted in the absence of any commercial or financial
278 relationships that could be construed as a potential conflict of interest.

AUTHOR CONTRIBUTIONS

279 MH and QJ contributed to conception and design of the study. QJ organized the database. MH performed
280 the statistical analysis. MH wrote the first draft of the manuscript. All authors contributed to manuscript
281 revision, read, and approved the submitted version.

FUNDING

282 This publication is funded by the University of California Santa Barbara Open Access Publishing Fund.

ACKNOWLEDGMENTS

283 The authors gratefully acknowledge the support from Global Fishing Watch in providing parts of the data
284 and assisting with data analysis.

SUPPLEMENTAL DATA

285 Supplementary Material should be uploaded separately on submission, if there are Supplementary Figures,
286 please include the caption in the same file as the figure. LaTeX Supplementary Material templates can be
287 found in the Frontiers LaTeX folder.

DATA AVAILABILITY STATEMENT

288 The datasets generated this study can be found in the public github repository, <https://github.com/mhu48/SSM-on-fishing-effort>.

REFERENCES

- 290 [Dataset] (1967). Fisheries and aquaculture department, food and agriculture organization of the united
291 nations
- 292 [Dataset] (2018). Global fishing watch
- 293 [Dataset] (2019). Marine regions
- 294 Banzon, V., Smith, T. M., Steele, M., Huang, B., and Zhang, H.-M. (2020). Improved estimation of proxy
295 sea surface temperature in the arctic. *Journal of Atmospheric and Oceanic Technology* 37, 341 – 349.
296 doi:10.1175/JTECH-D-19-0177.1
- 297 Blangiardo, M. and M., C. (2015). *Spatial and spatio-temporal Bayesian models with R-INLA* (John Wiley
298 & Sons)
- 299 [Dataset] Douglas Nychka, Reinhard Furrer, John Paige, and Stephan Sain (2021). fields: Tools for spatial
300 data. R package version 14.1
- 301 Gall, R. J. (1885). Use of cylindrical projections for geographical astronomical, and scientific purposes.
302 *Scottish Geographical Magazine* 1, 119–123. doi:10.1080/14702548508553829

- 303 Godana, A. A., Mwalili, S. M., and Orwa, G. O. (2019). Dynamic spatiotemporal modeling of the infected
 304 rate of visceral leishmaniasis in human in an endemic area of amhara regional state, ethiopia. *PLOS*
 305 *ONE* 14, 1–21
- 306 [Dataset] Gribov, A. and Krivoruchko, K. (2018). New flexible compact covariance model on a sphere
 307 Hefley, T. J., Hooten, M. B., Hanks, E. M., Russell, R. E., and Walsh, D. P. (2017). Dynamic spatio-temporal
 308 models for spatial data. *Spatial Statistics* 20, 206–220
- 309 Lindström, J., Szpiro, A., Sampson, P., Oron, A., Richards, M., Larson, T., et al. (2014). A flexible
 310 spatio-temporal model for air pollution with spatial and spatio-temporal covariates. *Environmental and*
 311 *Ecological Statistics* 21, 411–433. doi:10.1007/s10651-013-0261-4
- 312 [Dataset] Porcu, E., Alegría, A., and Furrer, R. (2017). Modeling temporally evolving and spatially globally
 313 dependent data
- 314 Rue, H., Martino, S., and Chopin, N. (2009). Approximate bayesian inference for latent gaussian models
 315 by using integrated nested laplace approximations. *Journal of the Royal Statistical Society: Series B*
 316 (*Statistical Methodology*) 71, 319–392
- 317 Stroud, J. R., Müller, P., and Sansó, B. (2001). Dynamic models for spatiotemporal data. *Journal of the*
 318 *Royal Statistical Society: Series B (Statistical Methodology)* 63

FIGURES AND TABLES

Table 1. Variables of interest.

Variable name	Definition
<i>date</i>	A string in format YYYY-MM-DD
<i>lat_bin</i>	The southern edge of the grid cell, in 100ths of a degree, 101 is the grid cell with a southern edge at 1.01 degrees north
<i>lon_bin</i>	The western edge of the grid cell, in 100ths of a degree, 101 is the grid cell with a western edge at 1.01 degrees east
<i>flag</i>	The flag state of the fishing effort, in iso3 value
<i>fishing_hours</i>	Hours that vessels of this geartype and flag were fishing in this gridcell on this day

Table 2. Posterior estimates of parameters.

Parameter	Posterior estimates for east coast	Posterior estimates for west coast
σ_ξ^2	11212.49	2952.089
σ_γ^2	17.45	14.30
ρ	1.04	1.06
λ	0.85	0.89

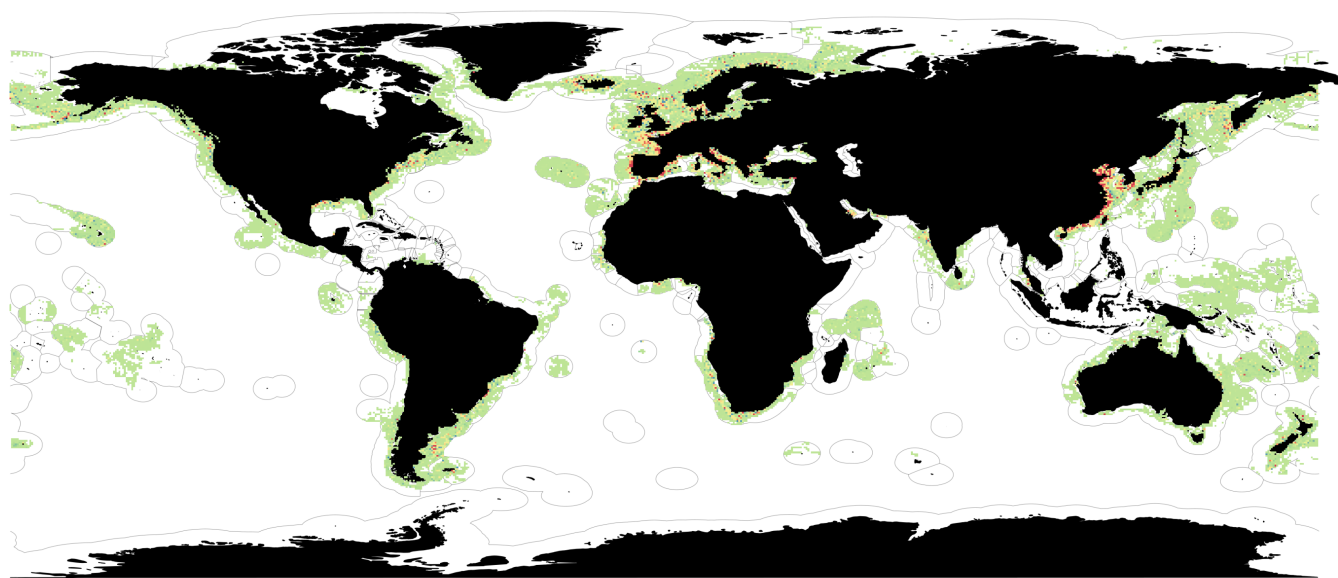


Figure 1. Global fishing effort in EEZ, 2018.

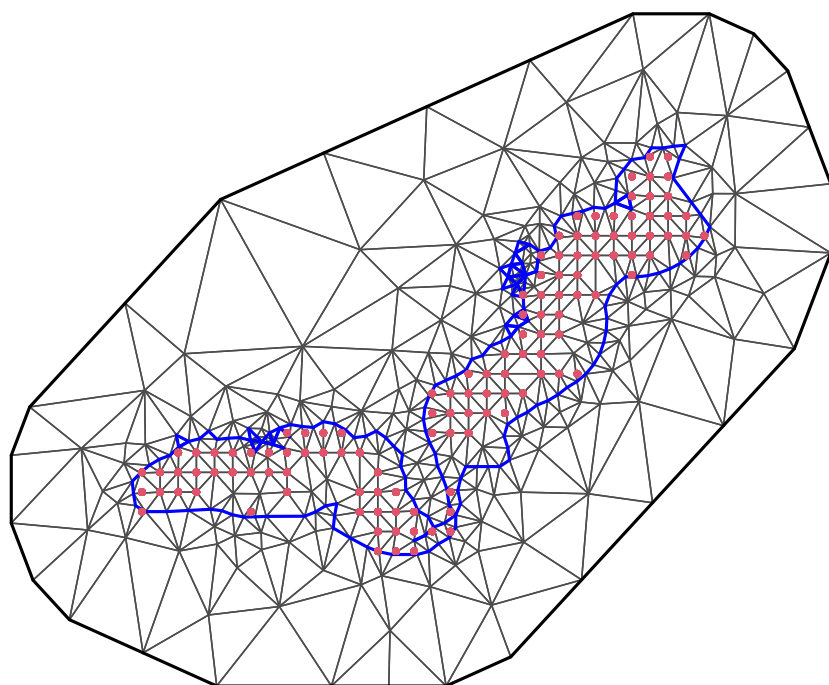


Figure 2. Triangulation of east coast EEZ.

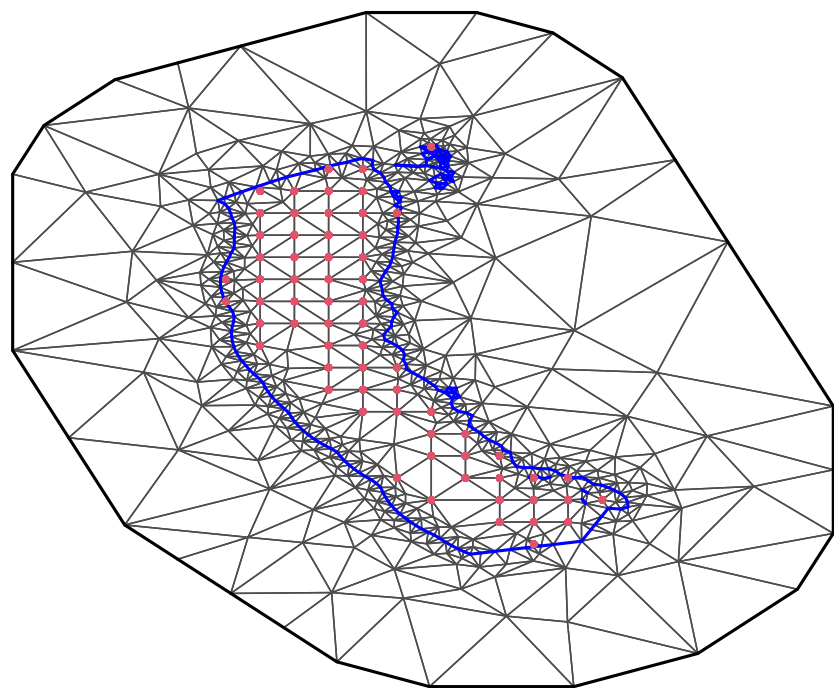


Figure 3. Triangulation of west coast EEZ.

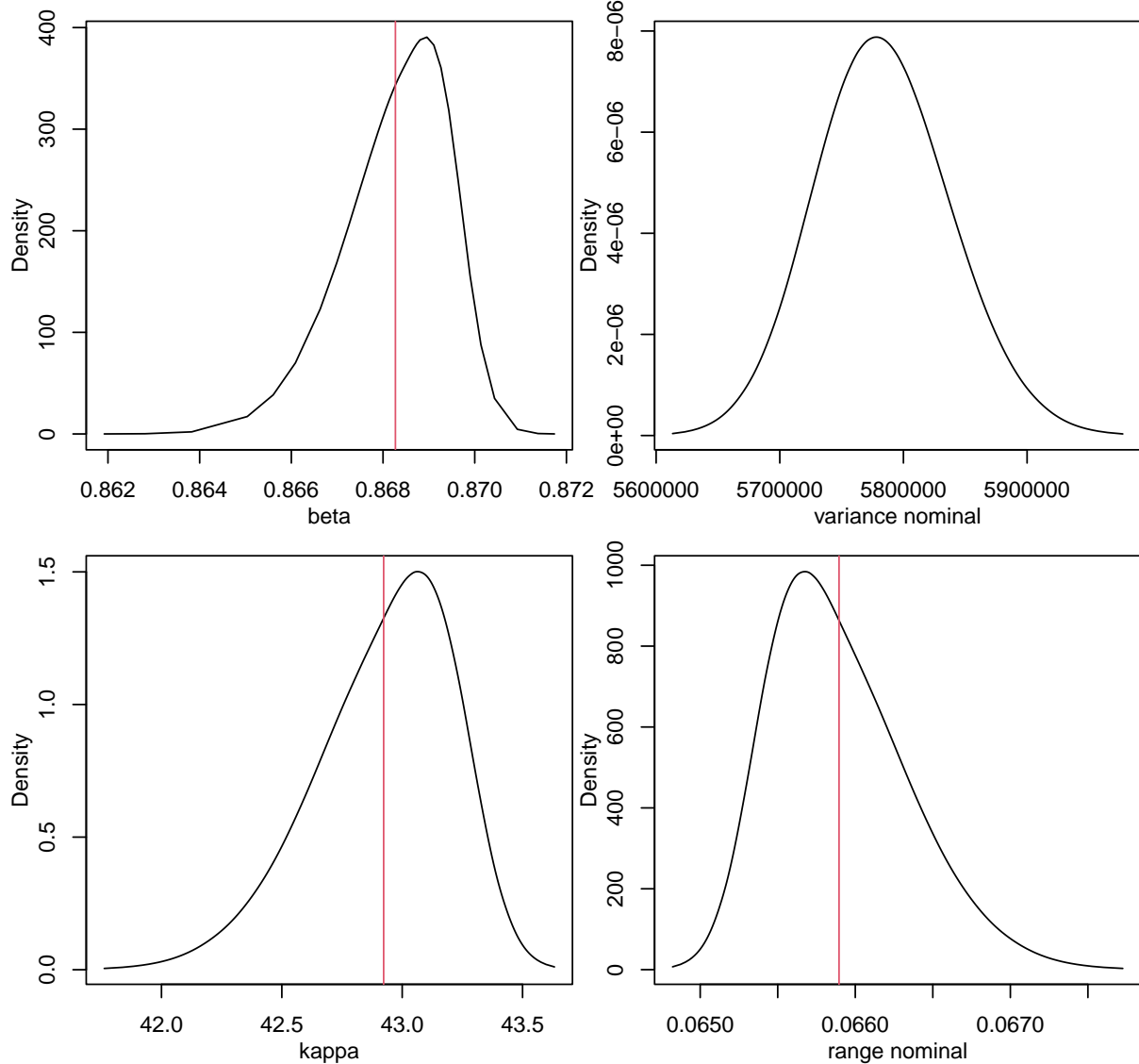


Figure 4. Posterior densities for east coast EEZ.

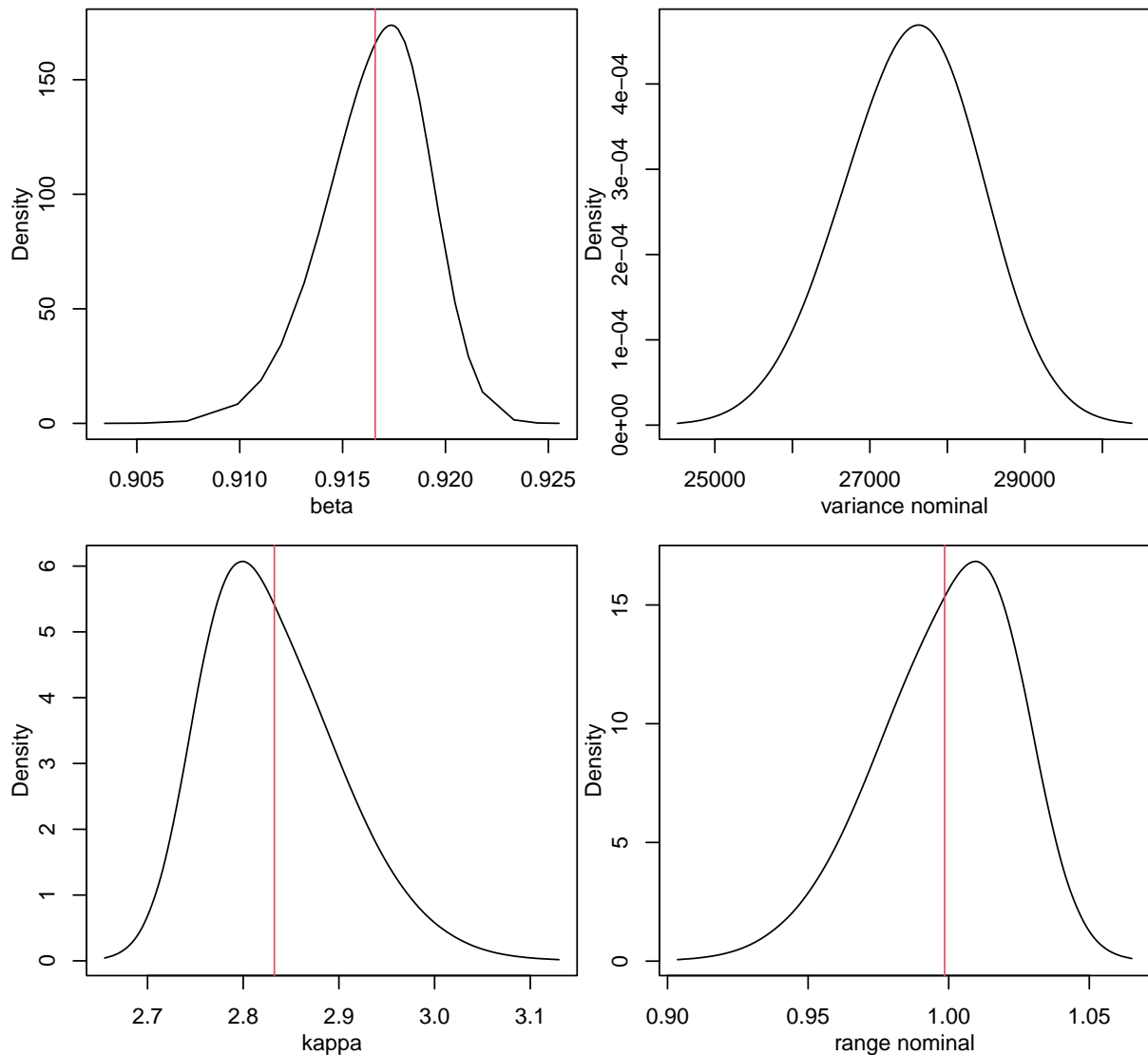


Figure 5. Posterior densities for west coast EEZ.

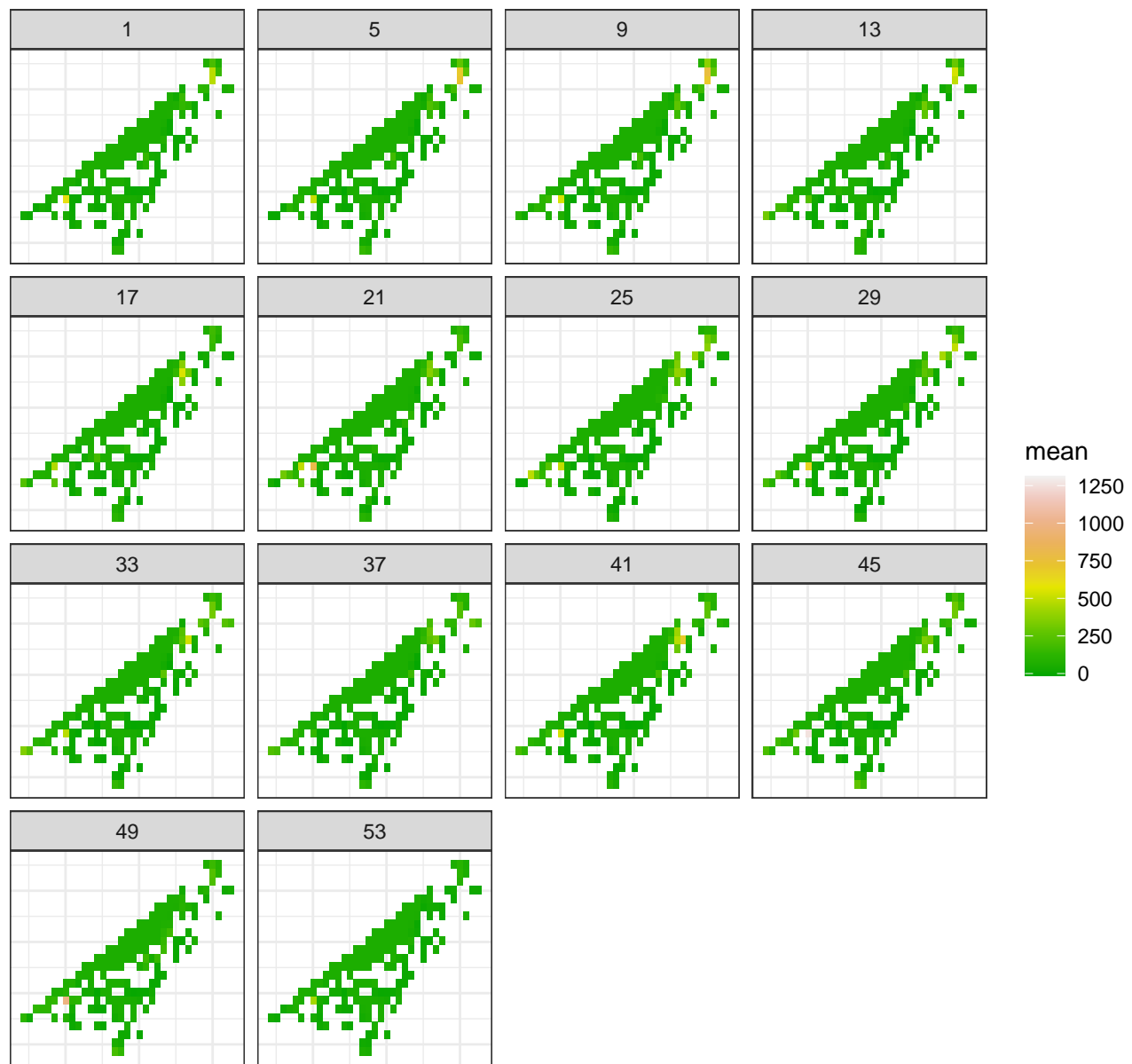


Figure 6. Predicted weekly fishing effort in east coast EEZ.

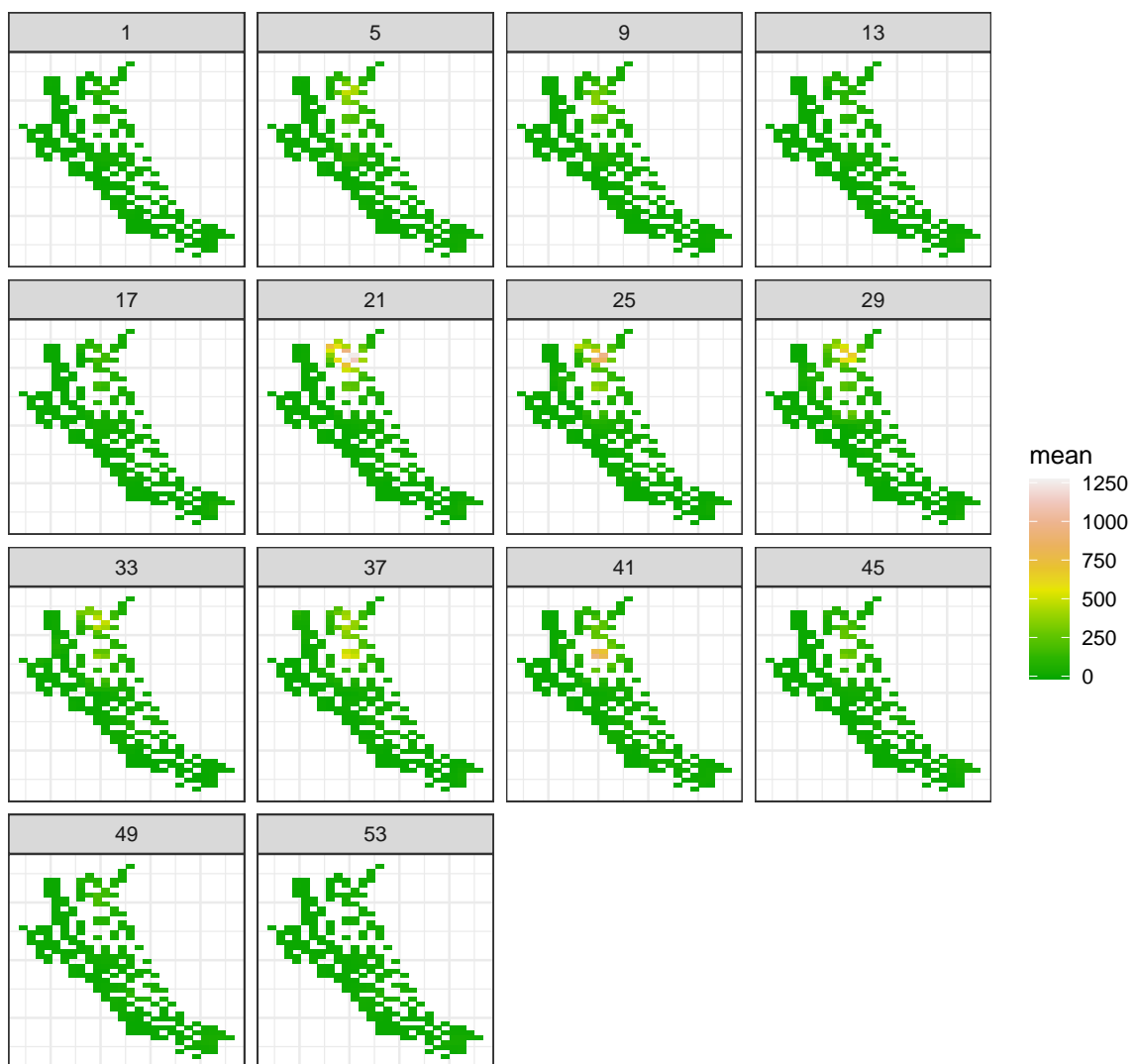


Figure 7. Predicted weekly fishing effort in west coast EEZ.